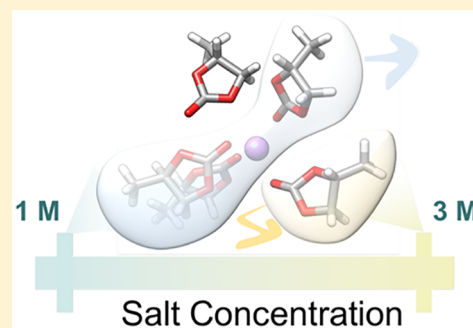


Transport in Superconcentrated LiPF₆ and LiBF₄/Propylene Carbonate Electrolytes

Julian Self,^{†,‡} Kara D. Fong,^{¶,‡} and Kristin A. Persson^{*,†,‡}[†]Department of Materials Science and Engineering, University of California, Berkeley, California 94720, United States[‡]Energy Technologies Area, Lawrence Berkeley National Laboratory, [¶]Department of Chemical and Biomolecular Engineering, University of California, Berkeley, California 94720, United States

Supporting Information

ABSTRACT: Superconcentrated electrolytes for lithium-ion batteries have shown promise in circumventing certain limitations of conventional carbonate electrolytes at lower concentrations while introducing new challenges such as decreased conductivity. We use molecular dynamics simulations with diffusion and residence time analyses to elucidate the main modes of transport of LiPF₆ and LiBF₄ in propylene carbonate at concentrations ranging from 1 to 3 M. Notably, we find that the Li⁺ mode of diffusion with respect to its surrounding propylene carbonate solvation shell is a mix of vehicular and structural diffusion at all studied concentrations, exhibiting a small increase toward structural diffusion in the superconcentrated regimes. Furthermore, and important for future strategies toward improved conductivity, we find that the Li⁺ ions associated with PF₆⁻ anions move in an increasingly vehicular manner as the salt concentration is increased, while the Li⁺ ions associated with BF₄⁻ anions move in an increasingly structural manner.



The liquid electrolyte of lithium-ion batteries (LIBs) provides a medium for ionic charge transport between the electrodes and effectively sets the window of electrochemical stability. Superconcentrated electrolytes for LIBs (~3 M) received attention as early as 1985^{1,2} and generally include both nonaqueous organic systems^{3–8} as well as aqueous electrolytes⁴ such as 3 M LiPF₆ in propylene carbonate (PC)^{3,6} or 21 m LiTFSI “water-in-salt”.⁴ Currently, both superconcentrated LiPF₆ in PC and superconcentrated LiBF₄ in PC (the latter with an added diluent) are under investigation as “state-of-the-art” electrolytes for LIBs.^{9–11} Interest in these systems stems from a combination of improved properties such as increased oxidative stability, absence of exfoliation, low volatility, higher charge density, and improved charge transfer kinetics.^{2,5} However, these potential advantages are not without drawbacks, as the cost of the salt is considerable, the viscosity may be dramatically increased, and the conductivity reduced. The impaired conductivity presents a fundamental flaw in particular, and considerable effort has been devoted to understanding the atomistic motifs for ionic conductivity in these complex, nondilute solutions with the aim to suggest possible improvements. Both structural as well as dynamic measurements have been employed, including nuclear magnetic resonance (NMR),^{6,12,13} infrared spectroscopy (IR),⁶ dielectric spectroscopy,¹⁴ and conductometric analysis¹³ as well as computational methods based on extensions of the mean spherical approximation (MSA) theory¹⁵ and molecular dynamics simulations.¹⁶ However,

despite the considerable body of work, there is no consensus on the molecular-level mechanisms of charge transport in superconcentrated aprotic electrolytes.² Yamada and Yamada² suggested that structural diffusion of Li⁺ may become the main transport mode as concentration is increased, perhaps due to a “repeated ion dissociation/association process”, as opposed to vehicular-type mechanisms that should dominate at lower concentrations. Such ion hopping processes are often referred to as Grotthus-type,¹⁴ where the hopping here refers to intersalt events, unlike the Grotthus-type processes that directly involve charge transfer to and from the solvent.^{17–19} Specifically for LiPF₆ in PC, Hwang et al.¹⁴ found via spectroscopy that contact dimers contribute to decreased conductivity in the high concentration regime and that the remaining conductivity is attributed to solvent separated ion pairs (SSIPs) and solvent separated dimers (SSDs). These authors found no support for any Grotthus-type ionic transport mechanism¹⁷ for LiPF₆ but suggested that Grotthus-type diffusion may be a possibility for LiBF₄ in PC in superconcentrated regimes. Adding to the debate regarding LiPF₆ in PC, Kondo et al.¹³ reported negligible ion-pairing (<20 %) via conductometric analysis even at high concentrations (>3 M). Hence, clarification of atomic level transport mechanisms is of immediate interest. In this work, we report the solvation

Received: September 26, 2019

Accepted: October 31, 2019

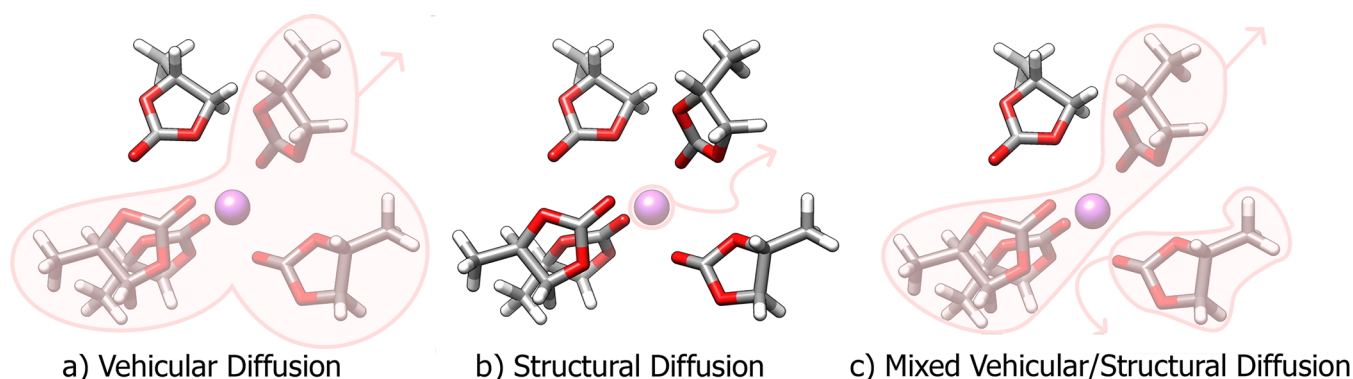


Figure 1. Cartoon illustration of diffusion of (a) vehicular quality, (b) structural quality, and (c) a mix of structural and vehicular quality. O, C, H, and Li atoms are shown as red, gray, white, and purple, respectively.

structure and diffusion constants of LiPF_6 in PC and LiBF_4 in PC for a range of concentrations spanning 1–3 M. We compare the obtained values to previously reported experiments and, using residence time and bound time analysis, recover the characteristic diffusion length scales, allowing for a thorough characterization of the transport modes for the respective salt components Li^+ , PF_6^- , and BF_4^- as a function of concentration.

To qualify the main mode of diffusion of a species i relative to another species j , the characteristic diffusional length scale L_{ij}^c can be obtained from the diffusion constant of a species D_i and residence time between two species τ_{ij}^{res} via the following relationship:

$$L_{ij}^c = \sqrt{6D_i\tau_{ij}^{\text{res}}} \quad (1)$$

The main mode of diffusion can be simply determined by comparing L_{ij}^c to the length scale relevant to the solvation shell L^S . Provided a judicious choice of L^S is made, which we discuss later, the following criteria can be employed:

$$L_{ij}^c > L^S \text{ vehicular motion}$$

$$L_{ij}^c < L^S \text{ structural diffusion} \quad (2)$$

Under vehicular transport, the species in question diffuses appreciably with its neighbors. Figure 1a shows one cartoon example where a tightly bound solvation shell diffuses as one species.²⁰ In structural diffusion,^{20,21} the neighboring species do not diffuse together by any appreciable amount, as illustrated in Figure 1b. For example, the neighboring solvents are frequently exchanged as the solvated species diffuses with its shell or the species undergoes some type of hopping or Grotthus-type mechanism. In Figure 1c, a mix of structural- and vehicular-type diffusion is shown, where a solvent is lost as the ion diffuses a distance comparable to the size of a solvation shell, while the remaining fraction of the solvation shell diffuses as a single kinetic entity.

D_i for both ions and solvent, can be obtained for a closed and thermally equilibrated liquid electrolyte system from the Einstein relation, provided the position \mathbf{x}_i of species i is known as a function of time:^{20,22}

$$D_i = \lim_{t \rightarrow \infty} \frac{1}{6t} \left\langle \frac{1}{N_i} \sum_i (\mathbf{x}_i(t) - \mathbf{x}_i(0))^2 \right\rangle \quad (3)$$

To determine the residence time τ_{ij}^{res} , or the average time species i and j travel together as neighbors before separating,

and subsequently extract a diffusion mechanism, it is necessary to define the relevant length scales for diffusion in the system. Two species (e.g., Li^+ and PC) are classified as direct neighbors if they are separated by a distance cutoff L^{cutoff} . In this work, L^{cutoff} is taken to be the minimum after the first peak of the relevant radial distribution function $g(r)$. The sizes of solvation shells, L^S , or alternatively, the distance between two solvation sites, is here shown in Table 1. Further details are provided in the Supporting Information.

Table 1. Size of Cutoff L^{cutoff} for Determination of Residence Times τ_{ij}^{res} and Estimate of Solvation Shell Size L^S between Two Species

	$\text{Li}^+\text{-PC}$ (Å)	$\text{Li}^+\text{-PF}_6^-$ (Å)	$\text{Li}^+\text{-BF}_4^-$ (Å)
L^{cutoff}	3.2	4.6	4.1
L^S	6.6	4.6	4.1

A residence time function $H(t)$ can be established such that $H(t)$ is unity if the two species are within L^{cutoff} of each other and zero otherwise.

$$H_{ij}(t) = \begin{cases} 1, & \text{if } \mathbf{x}_i(t) - \mathbf{x}_j(t) < L^{\text{cutoff}} \\ 0, & \text{otherwise} \end{cases} \quad (4)$$

The autocorrelation function of $H(t)$ can be then calculated:

$$\xi_{ij}(t) = \langle H_{ij}(t)H_{ij}(0) \rangle \quad (5)$$

From the autocorrelation function $\xi_{ij}(t)$, a biexponential fit²³ allows for inspection of the residence time τ_{ij}^{res} defined via the following relationship:

$$\xi_{ij}(t) = a \exp\left(\frac{-t}{\tau_{ij}^{\text{res}}}\right)^\beta + (1 - a) \exp\left(\frac{-t}{\tau_{ij}^{\text{short}}}\right) \quad (6)$$

In eq 6, a , τ_{ij}^{res} , τ_{ij}^{short} , and β are fitting parameters. The second term with τ_{ij}^{short} is ascribed to processes deemed subdiffusive, while the first term is relevant to the time scale of the diffusion process(es). β , the exponential stretch parameter ($0 < \beta \leq 1$), would deviate from unity as various diffusion modes of different time scales contribute to $\xi_{ij}(t)$.^{24,25} We note that this equation is similar to that used by Borodin and Smith²¹ and Dong et al.²⁶ for residence time analysis, where only the first term from the right-hand side is included: for $t \gg \tau_{ij}^{\text{short}}$, their employed equation is recovered. The more elaborate eq 6 is used here as the previous approximation^{26,27} does not explicitly

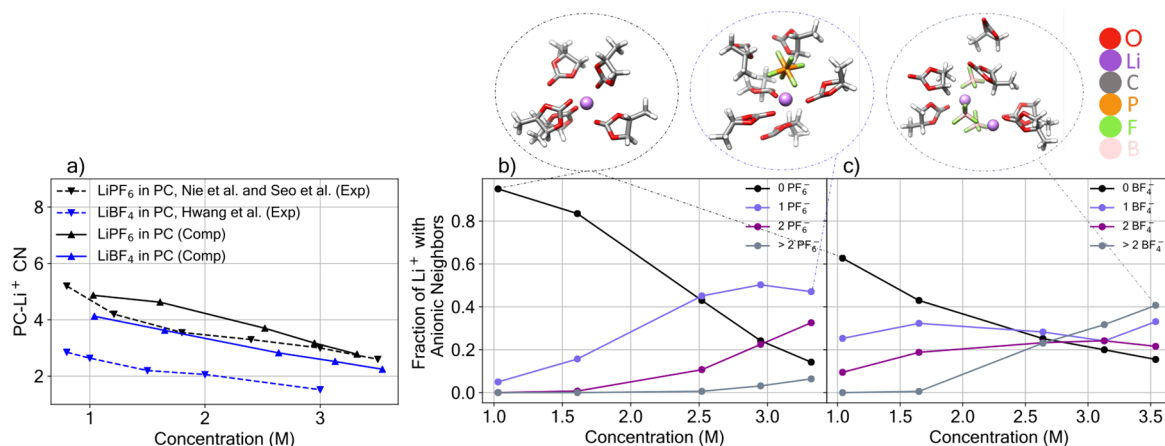


Figure 2. (a) CN of Li⁺ with PC computed in the present work and compared to available experimental values. (b) Fraction of Li⁺ with n PF₆⁻ counterions within L^{cutoff} computed in the present work. (c) Fraction of Li⁺ with n BF₄⁻ counterions within L^{cutoff} computed in the present work. Error bars for computed values are smaller than the data symbols used. Representative solvation structures are shown in the circles above.

yield a measure of the short time scales implied by including the fit from the first (stretched exponential) term alone. Thus, with eqs 1, 3, and 6, the condition in eq 2 qualifies the main diffusional mode of a species as either structural or vehicular. Note that the computed L_{ij}^c will depend on which species is assigned as species i and which is species j , i.e. which species' diffusion coefficient is used in eq 1. Here, we choose Li⁺ to be species i for all analyses.

As Li⁺ diffuses, it may move from one solvation shell with a counterion to another solvation shell with a different counterion. A measure of the time Li⁺ spends around at least one counteranion is the bound time τ^{bound} .²⁸ If the cation “hops” from one anion to another, it remains bound through multiple residence times for a total time τ^{bound} . Such a measure is deemed useful to determine “ion-hopping” behavior. τ^{bound} was calculated using the average time the primary solvation shell of a Li-ion includes at least one anion with a smoothing function which removes events on a time scale smaller than $\tau_{\text{PC-Li}^+}^{\text{short}}$ to avoid including subdiffusive events.

Molecular dynamics simulations were carried out with GROMACS (GROningen MACHine for Chemical Simulations).²⁹ Initial configurations were packed with PACKMOL in box sizes of $5 \times 5 \times 5 \text{ nm}^3$.³⁰ Five different concentrations between 1.0 and 3.6 M were studied for both LiPF₆ in PC and LiBF₄ in PC, respectively. Production runs were 50 ns for the two lowest concentrations and at least 100 ns for the three highest concentrations. These were under the isothermal–isobaric ensemble using a Parinello-Rahman³¹ barostat (4000 fs relaxation) with a velocity rescaling thermostat³² (1000 fs relaxation) with a 2 fs time step of integration for the equations of motion. The diffusion constants were obtained by inspecting the linear regime³³ of the time-averaged mean squared displacement of all relevant moieties (see Supporting Information for further details). Diffusion constants of Li⁺, PF₆⁻, and PC were calculated in this work using eq 3.

Force field parameters for PC and Li⁺ were taken from the standard OPLS force field,³⁴ while those for PF₆⁻ are taken from Lopez and Padua³⁵ and BF₄⁻ from Doherty et al.³⁶ Atom type identification and partial charge assignments for PC were automated using the Macromodel software package,³⁷ which generates charges based on the OPLS force field defaults using the bond-charge increment formalism.³⁸ Ionic charges for Li⁺

and PF₆⁻ were scaled by 0.8 as default charges (± 1.0) have been shown to typically overestimate interionic interactions in nonpolarizable force fields.^{39,40} We note previous work on MD simulations of LiPF₆ and LiBF₄ at conventional concentrations (1 M) which have not scaled down ionic charges have underestimated diffusivity constants by an order of magnitude, as well as overestimated ionic correlations.¹² Preceding the production runs, initial equilibrations were undertaken with a steepest descent, conjugate gradient minimization, followed by an isothermal–isobaric ($T = 298 \text{ K}$, $P = 1 \text{ atm}$) equilibration with the Berendsen barostat⁴¹ for 5 ns duration. Duplicate production runs were undertaken for all concentrations, and error bars report the standard error of the two duplicates.

Figure 2a shows the solvent coordination number (CN) of Li⁺ as a function of salt concentration. Analyzing CN informs us of solvation structure. Experimental values based on IR measurements from various groups for PC-LiPF₆ and PC-LiBF₄ have been plotted for comparison.^{6,14,42} The exact coordination number of Li⁺ in carbonate solutions is the subject of ongoing investigation,^{6,13,42–51} and for similar concentrations can vary depending on the method of investigation by numbers of 3.^{44,50,51} Our simulation results agree within 2 of the coordination numbers of Nie et al. and Hwang et al. across various concentrations.^{6,14} Intuitively, the coordination number decreases with concentration due to the increased number of neighboring anions as concentration is increased,⁵² in agreement with the experimental trends. Li⁺ in the LiBF₄ solution shows lower average coordination numbers due to increased ion-pairing over LiPF₆. Figures 2b and 2c show the average number of anionic neighbors of Li⁺. According to a strictly static structural criteria, Li⁺ with no neighboring anion is either a free ion⁵³ or part of a solvent-separated ion pair (SSIP),⁵³ whereas Li⁺ with one neighboring PF₆⁻ is part of a contact ion pair or a larger aggregate such as a positive triple ion. At 1.0 M, the most populous Li⁺ solvation shell is one with strictly PC molecules. For dilute solutions (e.g., $c \ll 1 \text{ M}$) where ion pairing can be neglected, the CN has been inferred by previous work to be either 4 or 5,^{13,14} whereas our simulations indicate a (dilute) limiting coordination number of 5. At concentrations above 2.5 M, the Li⁺ solvation shells with 1 anion are the most populous for LiPF₆, while for LiBF₄, larger aggregates structures (above 2 anions in the

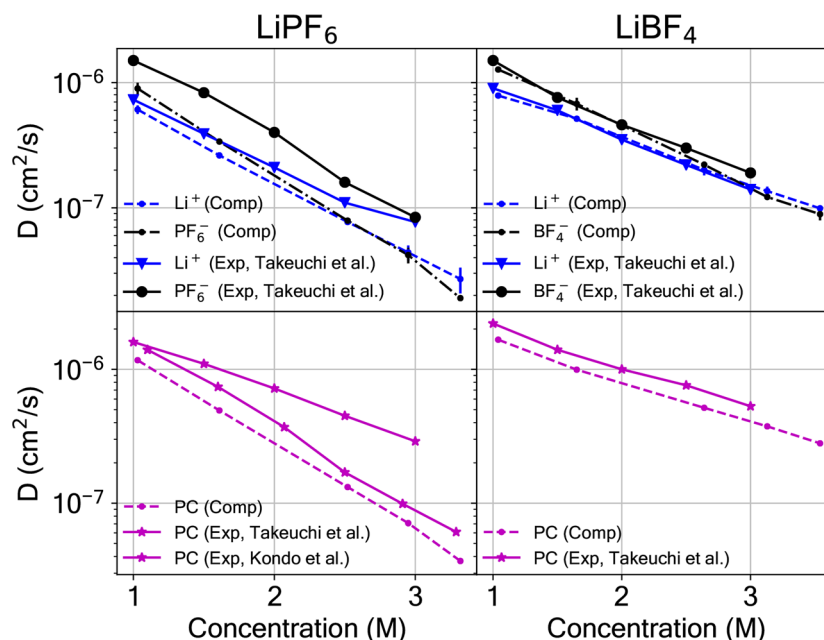


Figure 3. Diffusion constants as a function of salt concentration for ionic species (Li⁺, PF₆⁻, and BF₄⁻) (top row) and PC (bottom row) for LiPF₆ in PC (left column) and LiBF₄ in PC (right column). Experimental values are taken from the literature.^{12,13} Error bars, when smaller than the symbols for computed data, are not shown.

solvation shell) are favored. This strictly structural criterion does not properly consider whether or not ionic species form well-defined chemical entities with other ionic neighbors or alternatively exist as associated for a non-negligible duration in time. Such limitations of the strictly static criteria are overcome via a dynamical analysis such as those of ionicity (or Haven ratio), previously undertaken by Takeuchi et al.,¹² or analysis of the short-time diffusion mechanisms induced by ion complexation.⁵⁴ In this work, we undertake residence time analysis to investigate this dynamical behavior. Both ionicity and residence time analysis have been also used to study ionic liquids,²⁰ for which the aforementioned descriptions of ion correlation may be more apt than concepts of ion-pairing inferred via static structural measurements in dilute regimes.

To validate the dynamics of the simulations, diffusion constants were computed and compared to experiment. Figure 3 (top row) shows the computed diffusion constants as a function of concentration for the ionic species. The diffusion constants of all species decrease with increased salt concentration. However, there is a more pronounced decrease in the diffusion constant for the anions (PF₆⁻ or BF₄⁻) than for Li⁺. Thus, the ratio of $\frac{D_{\text{Li}^+}}{D_{\text{Li}^+} + D_{\text{anion}}}$, sometimes referred to as the transport number,⁵⁵ increases from 1 to 3 M. This trend is consistent with the experimentally reported values.¹² Figure 3 (bottom row) shows the PC solvent diffusion constant as a function of concentration. The diffusion constants for all three electrolyte species (Li⁺, PF₆⁻ or BF₄⁻, and PC) computed here are in fair agreement with the experimental results previously published.^{12,13} Hence, we surmise that the dynamics are well-reproduced by our models, which allows us to proceed to the residence time analysis.

Figure 4 (top panel) shows the residence time τ^{res} , which increases for all species as concentration is increased, consistent with an increase in viscosity.¹³ To distinguish the change in mode of diffusion, both the changes in τ^{res} and D must be accounted for. To this effect, values of τ^{res} and D allow

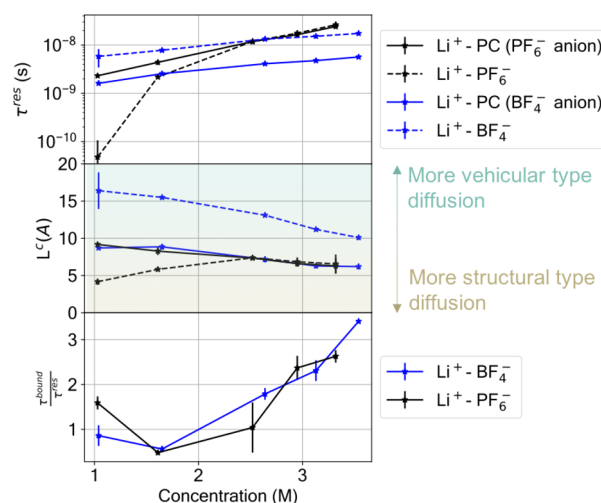


Figure 4. (top panel) Residence time τ^{res} for various species and (middle panel) L^c as a function of concentration. (bottom panel) $\frac{\tau^{\text{bound}}}{\tau^{\text{res}}}$. Error bars, when smaller than the symbols for computed data, are not shown.

calculation of L_{ij}^c via eq 1. Figure 4 (middle panel) shows L_{ij}^c as a function of concentration. $L_{\text{Li}^+ - \text{PC}}^c$ indicates that the transport mode of Li⁺ with PC for both anions is only slightly vehicular, and arguably mixed, as the solvent shell exchanges one of its comprising solvent molecules as the Li⁺ diffuses a distance slightly above a solvation shell size L^S (e.g., $\frac{L^c}{L^S} \approx 1.4$ at 1.0 M). At 1.0 M, Borodin and Smith found a similar result for LiTFSI in ethylene carbonate (i.e., $\frac{L^c}{L^S} \approx 1$),²¹ noting that this result is contrary to conventional expectation. For all concentrations studied here, the Li⁺ diffusion mode with respect to PC increases to slightly more structure diffusion-type as concentration increases.

The average transport mode of Li^+ with respect to neighboring PF_6^- at 1.0 M is a near equal mix of structural and vehicular motion ($\frac{L^c}{L^s} \approx 1$). However, as concentration is increased, the vehicular quality is significantly increased. This is in agreement with the experimental observation that the ionicity of LiPF_6 decreases with increasing concentration,¹² where positive and negative ions show a higher degree of correlation in their motion.

Analysis of the diffusion mode of Li^+ with respect to BF_4^- reveals that $L_{\text{Li}^+-\text{BF}_4^-}^c$ is significantly larger than $L_{\text{Li}^+-\text{PF}_6^-}^c$ in the studied concentration range, or more vehicular. In other words, a Li^+ will travel on average further with a BF_4^- than a PF_6^- . This can be rationalized by the stronger binding energy between Li^+ and BF_4^- than Li^+ and PF_6^- , a trend which has been observed previously using both experimental conductivity measurements⁵⁶ and quantum chemical calculations in carbonate blends.⁵⁷ Moreover, the concentration trends are different for LiBF_4 and LiPF_6 : $L_{\text{Li}^+-\text{BF}_4^-}^c$ decreases while $L_{\text{Li}^+-\text{PF}_6^-}^c$ increases with concentration. This indicates that the diffusion of Li^+ with BF_4^- is increasingly structural with increasing concentration. We speculate that the reason for this is due to the fact that Li^+ in the LiBF_4 system on average holds more anions in its solvation shell (see Figures 2b and c), and a Li^+ may interact more strongly to an anion if it is the only anion in its primary solvation shell.

To further characterize the mode of transport, bound time analysis was employed. As defined above, τ^{bound} is a measure of the time spent by Li^+ around at least one counterion, and a higher ratio of $\frac{\tau^{\text{bound}}}{\tau^{\text{res}}}$ indicates a higher likelihood of ion-hopping. Figure 4 (bottom) shows $\frac{\tau^{\text{bound}}}{\tau^{\text{res}}}$ versus concentration.

The similar trends show that $\frac{\tau^{\text{bound}}}{\tau^{\text{res}}}$ increases above 1.5 M for both LiPF_6 and LiBF_4 solutions. We cautiously label such behavior as increasingly “ion-hopping”-type, where the Li^+ more often moves directly between different anions without entering an intermediate, fully solvated state. We note that in the electrolytes studied here, the solvation sites are not fixed as in PEO^{58,59} or polyelectrolytes.^{28,60} Across concentrations, $\frac{\tau^{\text{bound}}}{\tau^{\text{res}}}$ is comparable for LiBF_4 and LiPF_6 , indicating that similar ion-hopping behavior increase is seen for both systems. This is likely due to nonspecific bulk concentration effects. Thus, with regards to neighboring counterions, the differences in transport between LiPF_6 and LiBF_4 solutions are not in the ion-hopping behavior but between the distance traveled by a Li^+ before an anion is exchanged, and how that distance changes with concentration (increases to become more vehicular for LiPF_6 and decreases to become more structural for LiBF_4). Furthermore, we note that at high concentrations, the conductivity of LiBF_4 in PC overtakes that of LiPF_6 in PC,¹³ which we speculate as due to the change in mode of diffusion. Further investigation of this effect is subject of future work.

In summary, we report the solvation structure, diffusion constants, and main transport mechanisms of LiPF_6 and LiBF_4 in PC for a range of concentrations spanning 1–3 M. While there is a small increase in structural diffusion quality for the positive charge carrier Li^+ with respect to the solvent, its main mode of transport remains mixed-vehicular even at 3 M for both LiPF_6 in PC and LiBF_4 in PC systems. These results challenge previous beliefs which hold that the transport mode of Li^+ with respect to the solvent should be predominantly

structural at high concentrations.² Moreover, via residence time analysis, we find that the transport of Li^+ with respect to the counterion is significantly different, namely more vehicular, for BF_4^- over PF_6^- . Although the ion-hopping quality of Li^+ with respect to the counterion is comparable between LiBF_4 and LiPF_6 solutions as concentration is increased, Li^+ with respect to BF_4^- shows a shift toward more structural-type diffusion, in contrast to LiPF_6 which shows more vehicular-type. We hope that our work may be used to inform and explore viable paths forward to enhance and explore the transport of Li^+ in superconcentrated PC electrolytes. For example, low viscosity cosolvents, which may be used to enhance hydrodynamic properties, remain to be investigated in their effect on diffusion mechanisms.

■ ASSOCIATED CONTENT

Supporting Information

The Supporting Information is available free of charge on the ACS Publications website at DOI: 10.1021/acsenergylett.9b02118.

Additional details on the simulations and analysis (PDF)

■ AUTHOR INFORMATION

Corresponding Author

*E-mail: kapersson@lbl.gov.

ORCID

Julian Self: 0000-0002-5486-9559

Kara D. Fong: 0000-0002-0711-097X

Notes

The authors declare no competing financial interest.

■ ACKNOWLEDGMENTS

This work was intellectually led by the Battery Materials Research (BMR) program under the Assistant Secretary for Energy Efficiency and Renewable Energy, Office of Vehicle Technologies of the U.S. Department of Energy, Contract DE-AC02-05CH11231. This research used resources of the National Energy Research Scientific Computing Center (NERSC). K.D.F. acknowledges support from NSF GRFP under Grant DGE 1752814. We thank Dr. Sang-Won park for valuable discussion.

■ REFERENCES

- (1) McKinnon, W. R.; Dahn, J. R. How to Reduce the Intercalation of Propylene Carbonate in Li_xZrS and Other Layered Compounds. *J. Electrochem. Soc.* **1985**, *3*, 364.
- (2) Yamada, Y.; Yamada, A. Review—Superconcentrated Electrolytes for Lithium Batteries. *J. Electrochem. Soc.* **2015**, *162*, A2406–A2423.
- (3) Ding, Y.; Yun, J.; Liu, H.; Wan, Z.; Shen, M.; Zhang, L.; Qu, Q.; Zheng, H. A Safe and Superior Propylene Carbonate-Based Electrolyte with High-Concentration Li Salt. *Pure Appl. Chem.* **2014**, *86*, 585–591.
- (4) Suo, L.; Borodin, O.; Gao, T.; Olguin, M.; Ho, J.; Fan, X.; Luo, C.; Wang, C.; Xu, K. Water-in-Salt Electrolyte Enables High-Voltage Aqueous Lithium-Ion Chemistries. *Science* **2015**, *350*, 938–943.
- (5) Zheng, J.; Lochala, J. A.; Kwok, A.; Deng, Z. D.; Xiao, J. Research Progress towards Understanding the Unique Interfaces between Concentrated Electrolytes and Electrodes for Energy Storage Applications. *Advanced Science* **2017**, *4*, 1700032.
- (6) Nie, M.; Abraham, D. P.; Seo, D. M.; Chen, Y.; Bose, A.; Lucht, B. L. Role of Solution Structure in Solid Electrolyte Interphase

- Formation on Graphite with LiPF₆ in Propylene Carbonate. *J. Phys. Chem. C* **2013**, *117*, 25381–25389.
- (7) Kim, Y.-S.; Jeong, S.-K. Raman Spectroscopy for Understanding of Lithium Intercalation into Graphite in Propylene Carbonated-Based Solutions. *J. Spectrosc.* **2015**, *2015*, 1–5.
- (8) Petibon, R.; Aiken, C.; Ma, L.; Xiong, D.; Dahn, J. The Use of Ethyl Acetate as a Sole Solvent in Highly Concentrated Electrolyte for Li-Ion Batteries. *Electrochim. Acta* **2015**, *154*, 287–293.
- (9) Doi, T.; Masuhara, R.; Hashinokuchi, M.; Shimizu, Y.; Inaba, M. Concentrated LiPF₆/PC electrolyte solutions for 5-V LiNi_{0.5}Mn_{1.5}O₄ positive electrode in lithiumion batteries. *Electrochim. Acta* **2016**, *209*, 219–224.
- (10) Doi, T.; Shimizu, Y.; Hashinokuchi, M.; Inaba, M. Dilution of Highly Concentrated LiBF₄/Propylene Carbonate Electrolyte Solution with Fluoroalkyl Ethers for 5-V LiNi_{0.5}Mn_{1.5}O₄ Positive Electrodes. *J. Electrochem. Soc.* **2017**, *164*, A6412–A6416.
- (11) Yamada, Y.; Wang, J.; Ko, S.; Watanabe, E.; Yamada, A. Advances and Issues in Developing Salt-Concentrated Battery Electrolytes. *Nature Energy* **2019**, *4*, 269–280.
- (12) Takeuchi, M.; Kameda, Y.; Umabayashi, Y.; Ogawa, S.; Sonoda, T.; Ishiguro, S.-i.; Fujita, M.; Sano, M. Ion–Ion Interactions of LiPF₆ and LiBF₄ in Propylene Carbonate Solutions. *J. Mol. Liq.* **2009**, *148*, 99–108.
- (13) Kondo, K.; Sano, M.; Hiwara, A.; Omi, T.; Fujita, M.; Kuwae, A.; Iida, M.; Mogi, K.; Yokoyama, H. Conductivity and Solvation of Li⁺ Ions of LiPF₆ in Propylene Carbonate Solutions. *J. Phys. Chem. B* **2000**, *104*, 5040–5044.
- (14) Hwang, S.; Kim, D.-H.; Shin, J. H.; Jang, J. E.; Ahn, K. H.; Lee, C.; Lee, H. Ionic Conduction and Solution Structure in LiPF₆ and LiBF₄ Propylene Carbonate Electrolytes. *J. Phys. Chem. C* **2018**, *122*, 19438–19446.
- (15) Gering, K. L. Prediction of Electrolyte Conductivity: Results from a Generalized Molecular Model Based on Ion Solvation and a Chemical Physics Framework. *Electrochim. Acta* **2017**, *225*, 175–189.
- (16) Ravikumar, B.; Mynam, M.; Rai, B. Effect of Salt Concentration on Properties of Lithium Ion Battery Electrolytes: A Molecular Dynamics Study. *J. Phys. Chem. C* **2018**, *122*, 8173–8181.
- (17) Grotthuss, C. J. T. *Mémoire sur la Décomposition de l'Eau et des Corps qu'Elle Tient en Dissolution à l'Aide de l'Electricité Galvanique*; 1805.
- (18) Rubinstein, I.; Bixon, M.; Gileadi, E. Confirmation of the Hopping Mechanism of the Conductivity of Bromide Ions in Solutions Containing Bromine. *J. Phys. Chem.* **1980**, *84*, 715–721.
- (19) Agmon, N. The Grotthuss Mechanism. *Chem. Phys. Lett.* **1995**, *244*, 456–462.
- (20) Solano, C. J. F.; Jeremias, S.; Paillard, E.; Beljonne, D.; Lazzaroni, R. A Joint Theoretical/Experimental Study of the Structure, Dynamics, and Li⁺ Transport in Bis([tri]fluoro[methane]-sulfonyl)imide [T]FSI-Based Ionic Liquids. *J. Chem. Phys.* **2013**, *139*, No. 034502.
- (21) Borodin, O.; Smith, G. D. LiTFSI Structure and Transport in Ethylene Carbonate from Molecular Dynamics Simulations. *J. Phys. Chem. B* **2006**, *110*, 4971–4977.
- (22) Frenkel, D.; Smit, B. *Understanding Molecular Simulation: from Algorithms to Applications*; Academic Press: San Diego, 2002; Vol. 1.
- (23) Rumble, C. A.; Uitvlugt, C.; Conway, B.; Maroncelli, M. Solute Rotation in Ionic Liquids: Size, Shape, and Electrostatic Effects. *J. Phys. Chem. B* **2017**, *121*, 5094–5109.
- (24) Anderssen, R. S.; Edwards, M. P.; Husain, S. A.; Loy, R. J. Sums of Exponentials Approximations for the Kohlrausch Function. 19th International Congress on Modelling and Simulation (Modsim 2011). 2011; p 7.
- (25) Kremer, F.; Schönhals, A., Eds. *Broadband Dielectric Spectroscopy*; Springer Berlin Heidelberg: Berlin, Heidelberg, 2003.
- (26) Dong, D.; Sälzer, F.; Røling, B.; Bedrov, D. How Efficient is Li⁺ Ion Transport in Solvate Ionic Liquids Under Anion-Blocking Conditions in a Battery? *Phys. Chem. Chem. Phys.* **2018**, *20*, 29174–29183.
- (27) Borodin, O.; Smith, G. D. Mechanism of Ion Transport in Amorphous Poly(ethylene oxide)/LiTFSI from Molecular Dynamics Simulations. *Macromolecules* **2006**, *39*, 1620–1629.
- (28) Ma, B.; Nguyen, T. D.; de la Cruz, M. O. Control of Ionic Mobility via Charge Size Asymmetry in Random Ionomers. **2019**, arXiv: 1907.03946.
- (29) Abraham, M. J.; Murtola, T.; Schulz, R.; Páll, S.; Smith, J. C.; Hess, B.; Lindahl, E. GROMACS: High Performance Molecular Simulations Through Multi-Level Parallelism from Laptops to Supercomputers. *SoftwareX* **2015**, *1–2*, 19–25.
- (30) Martínez, L.; Andrade, R.; Birgin, E. G.; Martínez, J. M. PACKMOL: A Package for Building Initial Configurations for Molecular Dynamics Simulations. *J. Comput. Chem.* **2009**, *30*, 2157–2164.
- (31) Parrinello, M.; Rahman, A. Polymorphic Transitions in Single Crystals: A New Molecular Dynamics Method. *J. Appl. Phys.* **1981**, *52*, 7182–7190.
- (32) Bussi, G.; Donadio, D.; Parrinello, M. Canonical Sampling Through Velocity Rescaling. *J. Chem. Phys.* **2007**, *126*, No. 014101.
- (33) Kowsari, M. H.; Alavi, S.; Najafi, B.; Gholizadeh, K.; Dehghanpisheh, E.; Ranjbar, F. Molecular Dynamics Simulations of the Structure and Transport Properties of TetraButylphosphonium Amino Acid Ionic Liquids. *Phys. Chem. Chem. Phys.* **2011**, *13*, 8826.
- (34) Jorgensen, W. L.; Maxwell, D. S.; Tirado-Rives, J. Development and Testing of the OPLS All-Atom Force Field on Conformational Energetics and Properties of Organic Liquids. *J. Am. Chem. Soc.* **1996**, *118*, 11225–11236.
- (35) Canongia Lopes, J. N.; Pádua, A. A. H. Molecular Force Field for Ionic Liquids Composed of Triflate or Bistriflylimide Anions. *J. Phys. Chem. B* **2004**, *108*, 16893–16898.
- (36) Doherty, B.; Zhong, X.; Gathiaka, S.; Li, B.; Acevedo, O. Revisiting OPLS Force Field Parameters for Ionic Liquid Simulations. *J. Chem. Theory Comput.* **2017**, *13*, 6131–6145.
- (37) Mohamadi, F.; Richards, N. G. J.; Guida, W. C.; Liskamp, R.; Lipton, M.; Caufield, C.; Chang, G.; Hendrickson, T.; Still, W. C. MacroModel - an Integrated Software System for Modeling Organic and Bioorganic Molecules Using Molecular Mechanics. *J. Comput. Chem.* **1990**, *11*, 440–467.
- (38) Halgren, T. A. Merck Molecular Force Field. I. Basis, Form, Scope, Parameterization, and Performance of MMFF94. *J. Comput. Chem.* **1995**, *30*.
- (39) Leontyev, I.; Stuchebrukhov, A. Accounting for Electronic Polarization in NonPolarizable Force Fields. *Phys. Chem. Chem. Phys.* **2011**, *13*, 2613.
- (40) Liu, H.; Maginn, E. A Molecular Dynamics Investigation of the Structural and Dynamic Properties of the Ionic Liquid 1-n-Butyl-3-Methylimidazolium Bis(trifluoromethanesulfonyl)imide. *J. Chem. Phys.* **2011**, *135*, 124507.
- (41) Berendsen, H. J. C.; Postma, J. P. M.; van Gunsteren, W. F.; DiNola, A.; Haak, J. R. Molecular Dynamics with Coupling to an External Bath. *J. Chem. Phys.* **1984**, *81*, 3684–3690.
- (42) Seo, D. M.; Reininger, S.; Kutcher, M.; Redmond, K.; Euler, W. B.; Lucht, B. L. Role of Mixed Solvation and Ion Pairing in the Solution Structure of Lithium Ion Battery Electrolytes. *J. Phys. Chem. C* **2015**, *119*, 14038–14046.
- (43) Bogle, X.; Vazquez, R.; Greenbaum, S.; Cresce, A. v. W.; Xu, K. Understanding Li⁺ – Solvent Interaction in Nonaqueous Carbonate Electrolytes with ¹⁷O NMR. *J. Phys. Chem. Lett.* **2013**, *4*, 1664–1668.
- (44) Castriota, M.; Cazzanelli, E.; Nicotera, I.; Coppola, L.; Oliviero, C.; Ranieri, G. A. Temperature Dependence of Lithium Ion Solvation in Ethylene Carbonate–LiClO₄ Solutions. *J. Chem. Phys.* **2003**, *118*, 5537–5541.
- (45) Smith, J. W.; Lam, R. K.; Sheardy, A. T.; Shih, O.; Rizzuto, A. M.; Borodin, O.; Harris, S. J.; Prendergast, D.; Saykally, R. J. X-Ray Absorption Spectroscopy of LiBF₄ in Propylene Carbonate: a Model Lithium Ion Battery Electrolyte. *Phys. Chem. Chem. Phys.* **2014**, *16*, 23568–23575.
- (46) Kameda, Y.; Umabayashi, Y.; Takeuchi, M.; Wahab, M. A.; Fukuda, S.; Ishiguro, S.-i.; Sasaki, M.; Amo, Y.; Usuki, T. Solvation

Structure of Li^+ in Concentrated LiPF_6 -Propylene Carbonate Solutions. *J. Phys. Chem. B* **2007**, *111*, 6104–6109.

(47) Morita, M.; Asai, Y.; Yoshimoto, N.; Ishikawa, M. A Raman Spectroscopic Study of Organic Electrolyte Solutions Based on Binary Solvent Systems of Ethylene Carbonate with Low Viscosity Solvents Which Dissolve Different Lithium Salts. *J. Chem. Soc., Faraday Trans.* **1998**, *94*, 6.

(48) Tsunekawa, H.; Narumi, A.; Sano, M.; Hiwara, A.; Fujita, M.; Yokoyama, H. Solvation and Ion Association Studies of LiBF_4 -Propylenecarbonate and LiBF_4 -Propylenecarbonate-Trimethyl Phosphate Solutions. *J. Phys. Chem. B* **2003**, *107*, 10962–10966.

(49) Barthel, J.; Buchner, R.; Wismeth, E. FTIR Spectroscopy of Ion Solvation of LiClO_4 and LiSCN in Acetonitrile, Benzonitrile, and Propylene Carbonate. *J. Solution Chem.* **2000**, *29*, 18.

(50) Jiang, B.; Ponnuchamy, V.; Shen, Y.; Yang, X.; Yuan, K.; Vetere, V.; Mossa, S.; Skarmoutsos, I.; Zhang, Y.; Zheng, J. The Anion Effect on Li^+ Ion Coordination Structure in Ethylene Carbonate Solutions. *J. Phys. Chem. Lett.* **2016**, *7*, 3554–3559.

(51) Skarmoutsos, I.; Ponnuchamy, V.; Vetere, V.; Mossa, S. Li^+ Solvation in Pure, Binary, and Ternary Mixtures of Organic Carbonate Electrolytes. *J. Phys. Chem. C* **2015**, *119*, 4502–4515.

(52) Flores, E.; Ávall, G.; Jeschke, S.; Johansson, P. Solvation Structure in Dilute to Highly Concentrated Electrolytes for Lithium-Ion and Sodium-Ion Batteries. *Electrochim. Acta* **2017**, *233*, 134–141.

(53) Marcus, Y.; Hefter, G. Ion Pairing. *Chem. Rev.* **2006**, *106*, 4585–4621.

(54) Masia, M.; Rey, R. Diffusion Coefficient of Ionic Solvation Shell Molecules. *J. Chem. Phys.* **2005**, *122*, No. 094502.

(55) Videa, M.; Xu, W.; Geil, B.; Marzke, R.; Angell, C. A. High Li^+ Self-Diffusivity and Transport Number in Novel Electrolyte Solutions. *J. Electrochem. Soc.* **2001**, *148*, A1352.

(56) Ue, M. Mobility and Ionic Association of Lithium Salts in a Propylene Carbonate-Ethyl Methyl Carbonate Mixed Solvent. *J. Electrochem. Soc.* **1995**, *142*, 2577.

(57) Ponnuchamy, V.; Mossa, S.; Skarmoutsos, I. Solvent and Salt Effect on Lithium Ion Solvation and Contact Ion Pair Formation in Organic Carbonates: A Quantum Chemical Perspective. *J. Phys. Chem. C* **2018**, *122*, 25930–25939.

(58) Webb, M. A.; Jung, Y.; Pesko, D. M.; Savoie, B. M.; Yamamoto, U.; Coates, G. W.; Balsara, N. P.; Wang, Z.-G.; Miller, T. F. Systematic Computational and Experimental Investigation of Lithium-Ion Transport Mechanisms in Polyester-Based Polymer Electrolytes. *ACS Cent. Sci.* **2015**, *1*, 198–205.

(59) Liyana-Arachchi, T. P.; Haskins, J. B.; Burke, C. M.; Diederichsen, K. M.; McCloskey, B. D.; Lawson, J. W. Polarizable Molecular Dynamics and Experiments of 1,2-Dimethoxyethane Electrolytes with Lithium and Sodium Salts: Structure and Transport Properties. *J. Phys. Chem. B* **2018**, *122*, 8548–8559.

(60) Fong, K. D.; Self, J.; Diederichsen, K. M.; Wood, B. M.; McCloskey, B. D.; Persson, K. A. Ion Transport and the True Transference Number in Nonaqueous Polyelectrolyte Solutions for Lithium Ion Batteries. *ACS Cent. Sci.* **2019**, *5*, 1250–1260.